MOLECULAR PHYSICS, 1996, VOL. 88, NO. 5, 1157–1171

On the equilibrium and time relaxation of a lattice gas in several boxes

By A. ACHAHBAR, P. L. GARRIDO and J. MARRO
Instituto Carlos I de Física Teórica y Computacional, and Departamentos de Física Aplicada y Moderna, Facultad de Ciencias, Universidad de Granada, 18071-Granada, Spain

(*Received 19 July 1994; accepted 29 September 1995*)

Lattice gases are investigated consisting of several boxes in which any particle interacts only with particles at its nearest neighbour sites within the same box, and particles can hop from one box to the other so that the total number is conserved. Two equal square lattices with attraction between particles in the same plane are simulated using the Monte Carlo method. While the equilibrium properties of this system are related simply to those for the plane, time relaxation differs. There are some interesting consequences, e.g., a consideration of two lattices may permit the more accurate determination of steady state properties in some cases, and novel phenomena may be exhibited. The nature of finite-size effects for low density is peculiar also. Further cases that exhibit interesting behaviour, even for one-dimensional boxes, are studied analytically by means of exact and mean-field solutions.

1. Introduction and definition of model

The lattice gas [1] and its variations are known to capture sometimes the essential cooperative physics in natural systems. Therefore, they may reproduce ideally in the computer many interesting phenomena [2] such as condensation, phase equilibrium and segregation, hydrodynamic flows, ionic conduction, crystal growth, and adsorption by surfaces. In practice, however, simulations are hampered by the fact that incorporating real features of natural systems into the models increases dramatically the computer time needed. Even restricting to the crudest qualitative approximation of reality, the time evolution of lattice gases towards ordered states is very slow if only particle diffusion, e.g., nearest-neighbour exchanges, are allowed which is often required on physical grounds. Thus, it seems interesting to consider further variations of the ordinary lattice gas that may improve both model versatility and computational efficiency.

The ordinary lattice gas consists of an sc lattice in d dimensions, $\mathbf{Z}^d$, with configurations $\sigma = \{\sigma_x; \mathbf{x} \in \mathbf{Z}^d\}$, where $\sigma_x = 0$(hole), or 1(particle). The (configurational) energy is given by

$$H(\sigma) = -4J \sum_{\mathrm{NN}} \sigma_x \sigma_y, \tag{1}$$

where the sum is over all pairs of nearest neighbour (NN) sites. Let $\rho \equiv |\lambda|^{-1} \sum_x \sigma_x$ be a density, $|\lambda|$ the number of lattice sites or volume, and $N = \sum_x \sigma_x$ the number of particles. The nature of the equilibrium states in this system, to be denoted λ hereafter, is well known. In the infinite-volume limit ($|\lambda| \to \infty$, $N \to \infty$, $\rho = $ const.), λ exhibits a critical point for $\rho = 1/2$ and $d \geqslant 1$ at temperature $T_{C,d} \geqslant 0$, where equality holds for

Table 1. The variation with density of the exact Onsager temperature $T_{\mathrm{coex},2}$ for the coexistence curve of $\lambda \equiv \Lambda_{2,0}$, and of the temperature T_C locating the onset of condensation in $\Lambda_{2,2}$ as estimated from the MC data (see section 2 for the interpretation of the differences between $T_{\mathrm{coex},2}(\rho)$ and $T_C(\rho)$ for low ρ).

ρ	$T_{\mathrm{coex},2}$	T_C
0·50	1	1
0·35	0·999986	~ 1
0·20	0·997	0·97
0·15	0·988	0·95
0·10	0·964	0·93

$d = 1$. For $d > 1$, one may have below $T_{C,d}$ coexistence of two phases, i.e., liquid of density $\rho_0(T)$ and gas of density $1 - \rho_0(T)$ such that $\rho = x\rho_0 + (1-x)(1-\rho_0)$, where x represents the liquid fraction. The onset of condensation, $x \geqslant 0$, then occurs at temperature $T_{\mathrm{coex},d}(\rho)$ which is the solution of $\rho_0(T) = 1 - \rho$; $T_{C,d} \equiv T_{\mathrm{coex},d}(\rho = 1/2)$; table 1 gives values for $T_{\mathrm{coex},2}(\rho)$. It is well established also that many properties of λ may be inferred from Monte Carlo (MC) studies for finite $|\lambda|$.

We report here on some results for equilibrium states and time relaxation in lattice gases with broken bonds. The most general system of interest, which we denote $\Lambda_{d,d',\cdots}$ (or, alternatively, Λ) is a sum of n adjacent disjoint lattice gases of dimension $d, d', \ldots$, respectively. That is, $\Lambda \equiv \bigcup_j \lambda_j$ with $\lambda_j \bigcap \lambda_k = \emptyset$ for any $j \neq k = 1, \ldots, n$; the volume is $|\Lambda| = \sum_j |\lambda_j|$; the configurations have energy

$$H_\Lambda(\sigma) = \sum_{j=1}^{n} H_j(\sigma^j). \tag{2}$$

For simplicity, $H_j(\sigma^j)$ is assumed to have the structure of equation (1) (unless otherwise indicated); $\sigma^j = \{\sigma_x; \mathbf{x} \in \mathbf{Z}^d\}$ represents a configuration of λ_j. The total number of particles is conserved,

$$N = \sum_j N_j = \sum_j \sum_{\mathbf{x} \in \lambda_j} \sigma_x = \text{const.}, \tag{3}$$

but N_j is not. The case of Λ with $n = 2$ is denoted $\Lambda_{d,d'}$ hereafter. It comprises two standard lattice gases, λ_1 and λ_2, of dimension d and d', respectively. The simplest visualization occurs for $d = d'$ and $|\lambda_1| = |\lambda_2|$ if one lattice is on top of the other. Then, $\Lambda_{d,0} \equiv \lambda$, and $\Lambda_{1,1}$ ($\Lambda_{2,2}$) consists of two linear (square) lattices such that any site has three (five) NN, with one of them in the other lattice, and $\Lambda_{3,3}$ consists of two cubes such that any site has six NN, with one of them in the other lattice if the given site belongs to one of the contact surfaces. Such correspondence between sites in different boxes does not occur if $|\lambda_1| \neq |\lambda_2|$, however. In general, we assume that the free (non-contact) surfaces of λ_1 and λ_2 go to infinity to obtain proper extensive properties; periodic (toroidal) boundary conditions are assumed, however, in computer studies which refer to finite systems $\Lambda_{2,2}$ of volume $|\Lambda| = 2|\lambda|$. In any case, equation (2) reads $H_\Lambda(\sigma) = H_1(\sigma^1) + H_2(\sigma^2)$ for $\Lambda_{2,2}$, i.e., any two particles interact only if located at NN sites such that both belong either to λ_1 or to λ_2, as if the bonds between λ_1 and λ_2 are broken ($J = 0$ between any two sites in different boxes). No further restrictions on the configurations of Λ are assumed; in particular, any given particle has access to any of the lattices.

We have studied $\Lambda_{d,d'}$ in some detail. It has an extra degree of freedom (particles can leave a given box), which is important from various points of view. In the first place, we mention that density fluctuations in Λ do not need to decay necessarily via diffusion in the same lattice. This may avoid the extremely slow evolutions that characterize λ, and helps us obtain good data in MC experiments. On the other hand, the different realizations of Λ provide an interesting background to the study of several problems. For example, the influence of spatial symmetries on critical behaviour, low dimensional ionic conduction, and surface and other phenomena in layered systems. Furthermore, Λ has allowed us a relatively easy study of phase coexistence, and this has promoted the active use during the last few years of the Gibbs ensemble, a computational procedure in which particles have access to several boxes (see, e.g., [3–8]). We believe that the present case, $\Lambda_{d,d'}$, is more natural and conceptually simpler, and also it seems more convenient in practice. As a matter of fact, we have been able to obtain some precise numerical results, and analytical results as well for some of the (simplest) cases of Λ. We mention the following features of our method which distinguish it from its predecessors: conserved quantities are the total number of particles and the volume of each box; one may have coexistence of phases within a box; configurations are related to each other by means of particle–hole exchanges, and the MC step is reasonably simple; it is feasible to simulate a relatively large system size; the density of each box does not fluctuate dramatically in general, e.g., it does not switch over during our experiments; there is no need for sampling within a restricted range of the order parmeter nor for restricting the value of the system density; one may approach reasonably critical and transition points; and the different lattices involved may differ essentially (e.g.) in dimension, volume, and interactions. Anyhow, the range of phenomena to which the present method can be applied is probably comparable to that for the Gibbs ensemble. Note that our system differs essentially from the case of two planes that are coupled by a local interlayer (two-spin) interaction [9].

The paper is organized as follows. In section 2 we report on the main results for the steady states of $\Lambda_{2,2'}$. In particular, MC data are shown to be consistent with simple hypothesis, and we explore the consequences of this. Section 3 refers to some interesting details of the time evolution of $\Lambda_{2,2'}$. In section 4 we describe briefly some general analytical facts for Λ, explicit exact results for $\Lambda_{1,1,\ldots}$, and mean-field theory for $\Lambda_{d,d'}$; it suggests, in particular, that some cases of $\Lambda_{d,d'}$ may exhibit rich, novel behaviour. A brief discussion of results is presented in section 5. The detailed MC study of $\Lambda_{2,2}$ subject to the (irreversible) action of an external driven dissipative electric field (cf. section 5) is reported elsewhere [10].

2. Interpretation of Monte Carlo data for steady states of $\Lambda_{2,2}$

We have studied $\Lambda_{2,2}$ by the MC method with the Metropolis algorithm. The data for $\rho \equiv |\Lambda|^{-1} \sum_x \sigma_x = 1/2$, where the sum is over the two planes, are for $|\Lambda| = 2|\lambda| = 9800$, while lattices with $|\Lambda| = 20\,000$ or more have been considered for $\rho = 0{\cdot}35$, $0{\cdot}2$, $0{\cdot}15$, and $0{\cdot}1$ (and smaller lattices for $\rho = 0{\cdot}05$ and $0{\cdot}01$ have been inspected qualitatively).

It is observed (figure 1) that $\Lambda_{2,2}$ segregates for $\rho = 1/2$ below a temperature T_C into liquid in one of the planes and gas in the other plane while the particles distribute homogeneously between the two planes above T_C. For $\rho < 1/2$, the phase segregation is qualitatively similar: a liquid cluster is in equilibrium for $T < T_C(\rho)$ in one of the

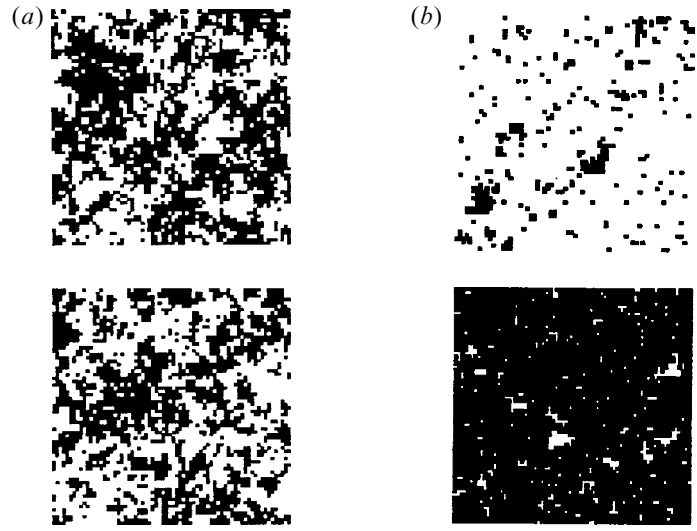

Figure 1. Typical stationary MC configurations in the two planes of $\Lambda_{2,2}$ with 9800 sites for $\rho = 1/2$: (*a*) $T = 1{\cdot}2T_{C,2} > T_C(\rho = 1/2)$, where $T_{C,2}$ represents the Onsager critical temperature, and (*b*) $T = 0{\cdot}95T_{C,2} < T_C(\rho = 1/2)$.

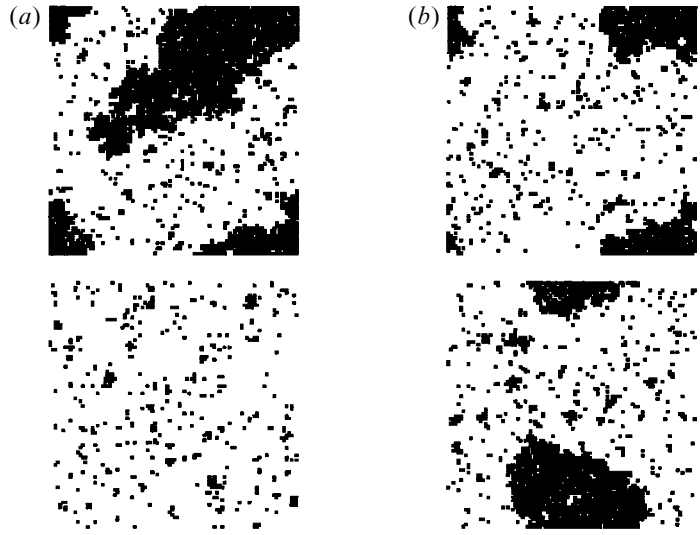

Figure 2. Typical MC configurations in the two planes of $\Lambda_{2,2}$ for $\rho = 0{\cdot}2$ at $T = 0{\cdot}9T_{C,2} < T_C(\rho = 0{\cdot}2)$: (*a*) in an equilibrium state, and (*b*) in a metastable-like but segregated state observed earlier during the same evolution.

planes with the gas, and the other plane is filled completely by gas; cf. figure 2(*a*). Such a condensation in only one of the planes is observed to be 'more stable' than the even distribution of the liquid phase between the two planes as in figure 2(*b*) (cf. below for a discussion of this fact). Moreover, it is observed that the densities $\rho_L(T)$ of the liquid and $\rho_G(T)$ of the gas phases are both apparently independent of ρ; compare the gas phase in figures 1(*b*) and 2(*a*), for instance.

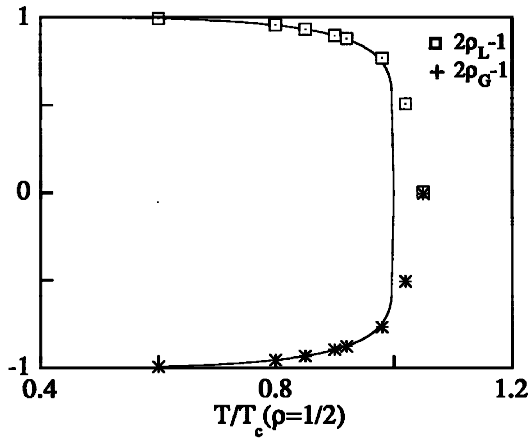

Figure 3. The density ρ_L of the liquid and ρ_G of the gas phases for $\rho = 1/2$ as a function of temperature in the MC experiments. See section 2 for an interpretation of the deviation from the Onsager solution (solid curve) observed here for $T > T_C$.

The above observations naturally lead us to assume that

$$\rho_L(T) = \rho_0(T), \quad \rho_G(T) = 1 - \rho_0(T), \tag{4}$$

where $\rho_0(T)$ is the Onsager solution for the condensed phase, i.e., $2\rho_0(T) - 1 = \{1 - [\sinh(2K)]^{-4}\}^{1/8}$, with $K \equiv J/k_B T$. In order to check for equation (4) directly, we have estimated $\rho_L(T)$ and $\rho_G(T)$ for $\rho = 1/2$ as the density within the plane holding the liquid and the gas, respectively. The result is shown in figure 3. It reveals perfect agreement with the Onsager solution for $T < T_{C,2}$ (the Onsager critical temperature) but not above $T_{C,2}$; in fact, T_C happens to equal $T_{C,2}$ for $\rho = 1/2$ (see below), and one may define $T_C(\rho = 1/2)$ as the temperature for which finite-size effects invalidate in practice our approximation $\rho_L(T) = \rho_1(T)$, $\rho_G(T) = \rho_2(T)$ (i.e., the densities of the two phases are evaluated simply by measuring the density within each plane during the stationary regime of the MC experiment).

If one admits that segregation occurs in one of the planes only, particle conservation (equation (3)) implies that

$$\rho = \tfrac{1}{2}\rho_G(T) + \tfrac{1}{2}[x\rho_L(T) + (1-x)\rho_G(T)], \tag{5}$$

and equation (4) leads to

$$x = 2(\rho - 1 + \rho_0)/(2\rho_0 - 1). \tag{6}$$

Thus, one has the same density in both planes, $\rho_1 = \rho_2 = \rho$, for $\rho < \rho_G(T)$, and it is required that $\rho \geqslant 1 - \rho_0(T)$ in order to have $x \geqslant 0$. In particular, the onset of condensation ($x = 0$) is characterized by $\rho = 1 - \rho_0(T)$ which is also the condition for the ordinary square lattice λ. Therefore, $\Lambda_{2,2}$ has the same coexistence curve as λ, $T_C(\rho) = T_{\mathrm{coex},2}$, and it also follows that $\Lambda_{2,2}$ has a critical point for $\rho = 1/2$ at $T_C(\rho = 1/2) = T_{C,2}$ which is of the Onsager class, namely, the order parameter critical exponent is $\beta = 1/8$.

Another interesting consequence of equations (4)–(6) is the following. Let us denote by $x_\Lambda = 2(\rho_\Lambda - 1 + \rho_0)/(2\rho_0 - 1)$ the fraction (equation (6)) of the liquid phase which is in one of the planes of $\Lambda_{2,2}$ when the overall density is ρ_Λ, and by $x_\lambda = (\rho_\lambda - 1 + \rho_0)/(2\rho_0 - 1)$ the corresponding quantity for the ordinary (square) lattice gas at density ρ_λ; $\rho_0 = \rho_0(T)$. Then, if the condensed plane of $\Lambda_{2,2}$ is to be equivalent to the

Onsager plane, one needs the relation $\rho_\Lambda = \frac{1}{2}[\rho_\lambda + \rho_G(T)] = \frac{1}{2}[\rho_\lambda + 1 - \rho_0(T)]$ between the respective densities.

In order to check for the general validity of equations (4)–(6), it is convenient to monitor the behaviour of a (non-conserved) order parameter defined as the difference in density between the two planes. This is simply related to the Onsager solution,

$$\Delta\rho(T) \equiv (2\rho)^{-1}|\rho_1(T) - \rho_2(T)| = \rho^{-1}|\rho - 1 + \rho_0(T)|, \tag{7}$$

and, consequently, to the difference in density between the phases. (Note that $\Delta\rho(T) = 0$ for $\rho < \rho_G(T)$, and $\Delta\rho(T) = \rho^{-1}[\rho - \rho_G(T)]$ for $\rho > \rho_G(T)$, for any T.) The actual density $\rho_i(T)$ in plane i ($= 1, 2$) at temperature T may be obtained in MC experiments as an average over stationary configurations. As expected, one observes that $\Delta\rho \to 1$ as $T \to 0$, $\Delta\rho \to 0$ as $T \to \infty$, and monotonic variation of $\Delta\rho$ with temperature. The data are fitted by equation (7) except for some peculiar finite-size effects (next paragraph). We observe, in particular, that $\Delta\rho$ remains continuous for any temperature and density. More precisely, on the assumption that $\Delta\rho \sim (T - T_{C,2})^\beta$ as $T \to T^-_{C,2}$ for $\rho = 1/2$, we have measured the Onsager value $\beta = 1/8$, and the data for $\rho \neq 1/2$ may be seen to be (roughly) consistent with the expectation $\Delta\rho \approx (1-\rho)\rho^{-1}[K_C \coth(2K_C)]/[1 - \sinh^4(2K_C)]\,\varepsilon$, where $K_C \equiv J/k_B T_C(\rho)$, which is obtained after writing $T = (1-\varepsilon)\,T_C(\rho)$ and expanding $\rho_0(T)$ around $\varepsilon = 0$. In practice, it is difficult to confirm the latter expectation numerically due to two facts. (1) The proportionality between $\Delta\rho$ and $T - T_C(\rho)$ is valid asymptotically only, and one may estimate that the region for which it is expected to hold varies dramatically with ρ and is rather small in general (e.g., the inverse of the proportionality coefficient is 0·18 for $\rho = 0{\cdot}10$ and less than 2×10^{-2} and 1×10^{-4} for $\rho = 0{\cdot}20$ and 0·35, respectively). (2) There is a peculiar finite-size effect for low ρ, as explained in the next paragraph. We have also monitored the behaviour of the energy, e.g., $E = E_1 + E_2$, where $E_i = |\lambda|^{-1}\,\eta_i^{+-}$, and η_i^{+-} represents the stationary mean number of particle–hole pairs in plane i. It follows that $|E_1 - E_2|$ is the lattice-gas interface energy given exactly by Onsager [11]. This is confirmed by the data, except for finite-size effects.

The table compares the (Onsager) coexistence curve which follows from the condition $\rho = 1 - \rho_0(T_C)$ and the temperature $T_C(\rho)$ for the onset of condensation in one of the planes that we have obtained numerically. The data are observed to deviate beyond typical MC errors and systematically from the Onsager solution $T_{\mathrm{coex},2}(\rho)$ as ρ is lowered. This is a peculiar effect related to the fact that one has $x_\Lambda(\rho) < x_\lambda(\rho)$ for *finite* systems at a given density because some particles of the liquid droplet in Λ need to go to the other plane to fill it with gas. Therefore, the onset of condensation ($x = 0$) occurs sooner for Λ than for λ as one increases the temperature for a given density. One may convince oneself that this effect is of the same order of magnitude as the differences reported in table 1, e.g., one may relate the coexistence curves as obtained from $x_\Lambda(\rho, T) = x_\lambda(\rho, T') = 0$. The reported (strong) dependence on ρ seems associated with the shape of $T_{\mathrm{coex},2}(\rho)$ which is very flat near $\rho = 1/2$ (where our MC estimates cannot be distinguished in practice from the Onsager solution). Of course, one has the usual finite-size effect adding to this. That is, the cost in surface tension for a small droplet is higher than the gain in bulk free energy; therefore, the system prefers remaining homogeneous until a larger droplet can be formed. As for the other effect, this implies that the onset of condensation in a finite system occurs at a lower temperature than for the corresponding infinite one, but it cannot explain the relatively large differences in table 1 for low ρ (incidentally, table 1 indicates that the error in our data near $\rho = 1/2$ due to this effect is also negligible).

Summing up, it seems undoubtedly that equation (4)–(6) is a solution for $\Lambda_{2,2}$; then, it corresponds to the (unique) equilibrium state for this problem [12]. (We give an extra argument in section 4 for this solution.) One may try to solve more complicated cases of Λ by following a similar procedure. In general, however, a previous MC study is required because the success of such a generalization based on intuition only is not guaranteed *a priori*. As an example, we mention the case $\Lambda_{2,1}$ that comprises a plane and a line (section 4); the situation may be even more involved for other cases of $\Lambda_{d,d,\ldots}$.

3. Some details of time evolution

The MC experiments have revealed also important differences in time evolution that suggests a peculiar relaxation of density fluctuations in Λ.

A typical evolution with time of (the absolute value of) $\Delta\rho$ in $\Lambda_{2,2}$ is presented in figure 4 for $\rho = 0{\cdot}2$. This illustrates one of the peculiarities of Λ which is more pronounced at low density. An early evolution (lasting up to $1{\cdot}5 \times 10^5$ MC steps, see caption to figure 4) occurs (case b of figure 4) in which the system might appear stationary with large fluctuations at first glance. This corresponds to the situation in which, in the absence of clustering, particles cannot get trapped in one of the planes. Once nucleation begins, $\Delta\rho$ evolves more monotonically. It becomes truly stationary, however, only after $4{\cdot}5 \times 10^5$ MC steps in the specific case b in figure 4. In fact, most of our evolutions run up to more than 10^6 MC steps. In any case, the stationary regime that we have considered for averages extends for more than 10^5 MC steps after both the onset of nucleation and the apparent equilibration with time of relevant quantities. We note that, after a net nucleation process sets in, an almost linear evolution towards full segregation occurs, and a stationary regime (in which the running average of, e.g., $\Delta\rho$ is constant) may be identified easily in practice after long times, as in cases a and b of figure 4 for $t > 2 \times 10^4$ and $t > 4{\cdot}5 \times 10^5$ MC steps, respectively.

Cases a and b of figure 4 differ from each other in the initial condition: the particles are initially evenly distributed between the two planes for b, while all the particles are initially in one of the planes for a. Therefore, figure 4 illustrates also the fact that one may obtain steady states rather economically (and very accurately) for $\Lambda_{2,2}$, as in case a of figure 4. This is in contrast to the situation for the ordinary lattice gas λ. That is, the slope of the time evolution curves for λ is typically non-zero (though it may be small in practice) in a comparable run, and fluctuations take a much larger time to become canonical (unlike in the present case, as revealed by the relatively good statistics of our data). The reason is that fluctuations need to decay via diffusion, which is an extremely slow process for ordered states with conserved density, while particles may search here for a hole in a given plane (for any $\rho \leqslant 1/2$) by means of hopping processes either in the other plane or from one plane to the other. This peculiarity of our system is illustrated further in figures 5 and 6. Figure 5 refers to the time evolution of the quantity [13]

$$m = [(M_y^{(\sin)})^2 + (M_y^{(\cos)})^2 + (M_x^{(\sin)})^2 + (M_x^{(\cos)})^2]^{1/2}, \tag{8}$$

where

$$M_y^{(\sin)} = \frac{\pi}{2L^2} \sum_{x=1}^{L} \sum_{y=1}^{L} \sigma_{\mathbf{r}} \sin\left(\frac{2\pi}{L} y\right), \tag{9}$$

etc.; here, $\mathbf{r} = (x, y)$ and $L^2 = |\lambda|$. Figure 6 depicts typical MC configurations. These

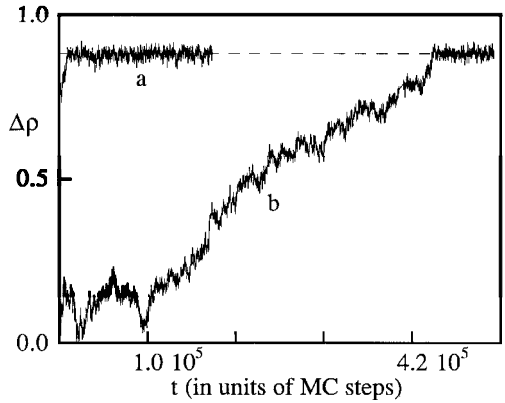

Figure 4. The variation with time of the order parameter $\Delta\rho$ in typical MC experiments for $\rho = 0{\cdot}2$ and $T = 0{\cdot}8T_{C,2} < T_C(\rho = 0{\cdot}2)$ and two different initial conditions (see text). A MC step is, rather arbitrarily, defined in this paper as the number of particle–hole NN pairs samples per lattice site; this is several times the standard unit for MC studies of the Ising model.

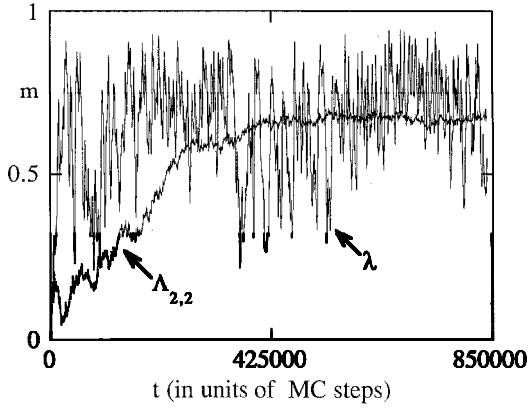

Figure 5. Typical variation with time in MC experiments of the order parameter m defined in equation (8) for both $\Lambda_{2,2}$ and λ, as indicated. The actual case here corresponds to $\rho = 0{\cdot}1$, $T = 0{\cdot}8T_{C,2}$, and $|\Lambda| = 20\,000$.

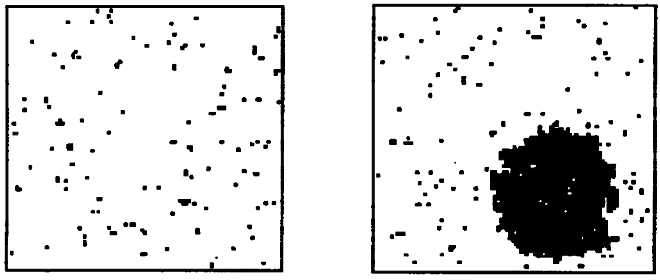

Figure 6. Typical configuration for the two planes of $\Lambda_{2,2}$ (corresponding to the experiment in figure 5) showing a compact cluster which cannot be obtained in a comparable time for λ.

figures, which are self-explanatory, suggest considerable significance for $\Lambda_{2,2}$; motivated by this, we are presently studying in more detail nucleation and spinodal decomposition phenomena in one of the planes of $\Lambda_{2,2}$.

We remark that, in spite of some apparent qualitative similarity (as described above), the cases $\rho < 1/2$ and $\rho = 1/2$ exhibit some essential differences. For example, quantities take a much longer time (as measured in MC time) to stabilize for $\rho \ll 1/2$ (e.g., for $\rho = 0{\cdot}2$) than for $\rho \approx 1/2$. It is a consequence in part of both the effect of the interface (which occurs only for $\rho < 1/2$) and the relative delay of nucleation as ρ becomes smaller, as compared with the earlier occurrence of spinodal decomposition for $\rho \approx 1/2$. Moreover, once segregation sets in, particles have for $\rho \ll 1/2$ a smaller probability of being captured by a cluster. Another distinct feature is the occurrence of metastable-like segregated states in some of the runs for $\rho < 1/2$ (while they never showed up for $\rho = 1/2$ in our experiments); cf. the example in figure 2(*b*). These have been observed to decay into states in which the liquid phase occurs in one of the planes only, and may not appear for given values of ρ and T when one uses a different seed for the random number generator or a different initial condition. We remark that these states are not strictly metastable (in the usual sense) given that a segregated phase exists, but they do not correspond to segregation in (only) one plane that seems to characterize the equilibrium low temperature behaviour of $\Lambda_{2,2}$. The states shown in figure 2(*a*, *b*) are both characterized by the same bulk free-energy density in the infinite-volume limit. However, the state in figure 2(*b*) has an extra surface energy which justifies the MC observation that it is not really stable. In fact, we show in the next section that such metastable-like states are consistent with the general formalism. This suggests again the prolific behaviour one may expect for different variations of Λ as compared with the relative simplicity of λ.

4. Further analytical results

In this section, we complement our observations above by deriving analytically some general conclusions. In particular, we show explicitly that equations (4)–(6) follow on the assumption that segregation with two coexisting phases occurs at a low enough temperature. We also discuss the case $\Lambda_{2,1}$, and obtain both exact and approximate results for some specific cases of Λ.

Consider the general system Λ of energy given by equation (2), total number of particles N, and total volume $|\Lambda|$, and $|\lambda_j|$ is the volume of box j (= $1, \ldots, n$). The partition function is

$$Z_\Lambda = \sum_{\sigma^1} \cdots \sum_{\sigma^n} \delta\left(N, \sum_{j=1}^{n} \sum_{x \in \lambda_j} \sigma_x\right) \exp\left[-\beta \sum_{k=1}^{n} H_k(\sigma^k)\right], \tag{10}$$

where $\delta(X, Y)$ represents the Kronecker delta function. Let us denote $\rho_j = N|\lambda_j|^{-1}$ the particle density for each box, and define the $(n-1)$-component vector $\vec{\rho} \equiv (\rho_1, \ldots, \rho_{n-1})$; ρ_n is not included in $\vec{\rho}$ but is determined by the given $\rho = N|\Lambda|^{-1}$. One gets near the thermodynamic limit for Λ (i.e., as $|\Lambda| \to \infty$, $N \to \infty$, and $|\lambda_j| \to \infty$ $\forall j$, with ρ and p_j $\forall j$ given finite constants) that

$$Z_\Lambda \approx \exp\left[-\beta |\Lambda| f(\beta, \vec{\rho}^*)\right], \tag{11}$$

where

$$f(\beta, \vec{\rho}) = \sum_{j=1}^{n-1} p_j f_j(\beta, \rho_j) + p_n f_n\left(\beta, p_n^{-1}\left[\rho - \sum_{j=1}^{n-1} p_j \rho_j\right]\right). \tag{12}$$

Here, $p_j \equiv |\lambda_j|\,|\Lambda|^{-1}$, and $\vec{\rho}^* = (\rho_1^*, \ldots, \rho_{n-1}^*)$ is the solution of $(\partial/\partial\rho_j) f(\beta, \vec{\rho})\big|_{\vec{\rho}=\vec{\rho}^*} = 0$ with $j = 1, \ldots, n-1$; more explicitly,

$$\frac{\partial f_j(\beta, \rho_j^*)}{\partial \rho_j^*} = \frac{\partial f_n(\beta, \rho')}{\partial \rho'}\bigg|_{\rho' = \frac{1}{p_n}\left[\rho - \sum_{j=1}^{n-1} p_j \rho_j^*\right]}, \quad j = 1, \ldots, n-1. \tag{13}$$

Stability requires that $g_{jk} = (\partial^2/\partial\rho_j^* \partial\rho_k^*) f(\beta, \vec{\rho}^*)$ is strictly positive, i.e., any eigenvalue of

$$g_{i_1 \cdots i_m} \equiv \frac{\partial^m f(\beta, \vec{\rho})}{\partial \rho_{i_1} \cdots \partial \rho_{i_m}}\bigg|_{\vec{\rho}=\vec{\rho}^*} \tag{14}$$

is positive for any m; $i_\alpha = 1, \ldots, n-1$, $\alpha = 1, \ldots, m$. Each set of values for β, ρ, and $p_j\ \forall j$ for which stability breaks down is a candidate for a critical point; the true equilibrium solution corresponds to the absolute minimum of $f(\beta, \vec{\rho}^*)$.

A few general results follow from the above. For example, consider a Hamiltonian (equation (2)) with identical terms H_j so that the free-energy density function is $f_j(\beta, \rho_j) = f(\beta, \rho_j)$ for all j. Assume further that $\rho_j^* = \rho$ for all j. This is a solution of equation (13), and the stability matrix is

$$g_{jk} = p_j (\partial^2/\partial\rho^2) f(\beta, \rho)\,[\delta(j,k) + p_k/p_n]. \tag{15}$$

This solution becomes marginal for $(\partial^2/\partial\rho^2) f(\beta, \rho) = 0$, as for λ with density ρ, as long as $\rho_j^* = \rho$ corresponds to an absolute minimum of $f(\beta, \vec{\rho}^*)$ (which may not be the case: see below). Then, the free-energy density for Λ is precisely $f(\beta, \rho)$, and both Λ and λ have the same phase above coexistence and the same critical behaviour approaching $T_{\mathrm{coex,d}}(\rho = 1/2)$ from above. Of course, this is far from implying that Λ behaves the same as λ in general. For example, $\rho_j^* = \rho$ does allow for inhomogeneities, and nothing is said about $\rho_j^* \neq \rho$. In fact, equation (12) suggests that $f(\beta, \vec{\rho}^*)$ characterizing Λ through equation (11) may contain richer behaviour than the box function $f(\beta, \rho)$, and the properties of Λ cannot be inferred straightforwardly from those of λ. The only simple general result seems to be that both systems have the same high temperature phase, but this is implied only for equal H_j's in as much as Λ is restricted to have $\rho_j = \rho$ for all j (and it corresponds to an absolute minimum of the free energy).

One may go one step further for some cases of Λ by combining the above with some extra information. We illustrate this fact by deriving the explicit solution (equations (1)–(3)) for $\Lambda_{2,2}$. Let us assume the existence of two coexisting phases within box λ_j. Then,

$$\lim_{l_j \to \infty} l_j (f_j(\beta, \rho_j) - f_j(\beta, \rho_j^*)) = S_j(x_j, \rho_j^*). \tag{16}$$

Here, ρ_j^* is a solution of $\partial f_j(\beta, \rho_j^*)/\partial\rho_j^* = 0$, x_j is the fraction of one of the phases in λ_j, i.e., $\rho_j = x_j \rho_j^* + (1 - x_j)(1 - \rho_j^*)$, S_j is the total surface free energy associated with the interface between the domains, and l_j represents the area of this interface (then, the last term of equation (16) is the interfacial tension per unit area). Thus, the extremum condition for $f(\beta, \vec{\rho}) = \sum_j p_j f_j(\beta, \rho_j)$ reduces for equation (16) to the condition of minimum global interface between the two phases. For $\Lambda_{2,2}$, this implies that $\rho_1 = x\rho_0 + (1 - x)(1 - \rho_0)$, $\rho_2 = \rho_0$.

The existence of a similar argument is not guaranteed in general. Consider, for example, $\Lambda_{2,1}$ consisting of a line λ_1 and a plane λ_2. It follows from equation (13) that

all the particles go to λ_2 at zero temperature. For a finite temperature, $\rho_1 < \rho_2$ because the binding energy is larger for the line than for the plane, which implies $\rho_2 > \rho$ and $\rho_1 < \rho$. For very high temperatures, $\rho_1 = \rho_2 = \rho$. That is, there is dependence of ρ_1 and ρ_2 on temperature which is *a priori* far from trivial and needs to be studied by solving explicitly $\partial f_1(\beta, \rho_1)/\partial \rho_1 = \partial f_2(\beta, \rho_2)/\partial \rho_2$ or equation (13). In fact, it would be interesting to reach a conclusion about the critical behaviour of $\Lambda_{2,1}$.

Next, we derive some specific exact and mean-field results for some versions of Λ. Consider first a combination of n one-dimensional lattices, $\Lambda_{1,1,\ldots}$ with $H_j(\sigma^j) = -4J_j \sum_x \sigma_x \sigma_{x+1} - h_j \sum_x \sigma_x, j = 1, \ldots, n$. Here, $h_j = -4J_j \forall j$ to have correspondence with the Ising model with zero field (and with the lattice gas at critical density). One obtains for f in equation (11):

$$\beta f(\beta, \vec{p}) = \sum_{j=1}^{n} p_j \left\{ -\beta h_j \rho_j + \rho_j \ln \left[\frac{4\rho_j(1-\rho_j)}{(\Delta_j - 2\rho_j + 1)^2} \right] + \ln \left[\frac{\Delta_j - 2\rho_j + 1}{\Delta_j + 1} \right] \right\}, \tag{17}$$

with $\rho = \sum_{j=1}^{n} p_j \rho_j$ and $\Delta_j^2 \equiv (2\rho_j - 1)^2 + 4\rho_j(1-\rho_j) X_j$ On the other hand,

$$(\Delta_j - 2\rho_j + 1)(\Delta_j + 2\rho_j - 1)^{-1} = (\Delta' - 2\rho' + 1)(\Delta' + 2\rho' - 1)^{-1}, \quad j = 1, \ldots, n-1, \tag{18}$$

corresponds to equation (13) for $h_j = -4J$; here,

$$\rho' = p_n^{-1} \left[\rho - \sum_{j=1}^{n-1} p_j \rho_j \right], \tag{19}$$

and Δ' is defined as Δ_j with ρ_j replaced by ρ'.

Let us consider $n = 2$, which is equivalent to a chain with $\rho = $ const. in which interactions are between next NN only. One may allow for different interactions within each box, i.e., $J_1 \neq J_2$, and for an unequal partition of the volume between the two lattices; hence, $p_1 \equiv u$ and $p_2 = 1 - u$. Then, equation (18) reduces to $\rho_1(1-\rho_1)(2\rho_2 - 1)^2 \exp(4\beta J_1) = \rho_2(1-\rho_2)(2\rho_1 - 1)^2 \exp(4\beta J_2)$. Some main facts for $\Lambda_{1,1}$ are as follows. For $\beta \to 0$, we may write for the density at each line:

$$\rho_1 = \rho + \beta(1-u)\varepsilon, \quad \rho_2 = \rho - \beta u \varepsilon, \quad \varepsilon = 4\rho(1-\rho)(2\rho - 1)(J_1 - J_2). \tag{20}$$

For $J_1 = J_2$, this reduces to the case $\rho_1 = \rho_2 = \rho$ at the beginning of the section. Otherwise, the chemical potential in the Hamiltonian induces a larger density for the line in which interactions are stronger (which favours the lowest energy). More explicitly, $\Delta\rho \equiv |\rho_1 - \rho_2| = 4\beta\rho(1-\rho)(2\rho - 1)(J_1 - J_2)$ for any u at a high enough temperature, i.e., only $\rho = 1/2$ corresponds to an even distribution of particles between the lines. For $\beta \to \infty$, one may write

$$\rho_1 = \rho_1^* + (1-u)\varepsilon'\gamma + O(\gamma^2), \quad \rho_2 = \rho_2^* - u\varepsilon'\gamma + O(\gamma^2). \tag{21}$$

Here, $\gamma \equiv \exp\{-4\beta(J_1 - J_2)\}$, we are assuming $J_1 > J_2$, and ρ_1^* and ρ_2^* are unknowns such that $\rho = u\rho_1^* + (1-u)\rho_2^*$. Consider $u = 1/2$ and $\rho < 1/2$ given the symmetry of the problem. It follows that $\rho_1^* = 0$, $\rho_2^* = 2\rho$, and $\varepsilon' = 4\rho(1-2\rho)(4\rho - 1)^{-2}$ is a solution for $\rho \leqslant 1/2$. In addition, $\rho_1^* = 2\rho - 1/2$, $\rho_2^* = 1/2$ is a solution for $\rho \geqslant 1/4$ (one needs to go to higher orders to find the corresponding expression for ε'). The general behaviour of ρ_1 and ρ_2 as a function of temperature is illustrated in figure 7 for different values of ρ and of the interactions. It may be understood as the result of competition at each T betwen the free energy functions for λ_1 and λ_2. Such an analysis and figure 7 suggest,

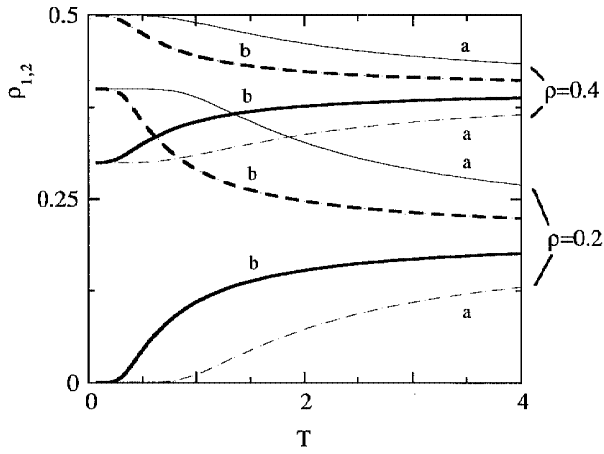

Figure 7. The variation with temperature ($J/k_B = 1$) of the density of particles, ρ_1 (solid curves) and ρ_2 (dashed curves), within the two linear lattices of $\Lambda_{1,1}$ for $J_2 = 1/2$, as given by the exact solution in section 4. The two lattices have the same volume fraction, $p_1 = p_2 = 1/2$. The upper set of four curves is for global density $\rho = 0{\cdot}4$, and the lower set is for $\rho = 0{\cdot}2$. The interaction strength for the other line is $J_1 = -1$ (curves labelled a) and 1 (curves labelled b).

in particular, that the mechanism which controls the behaviour at high T (cf. above) occurs here also but it competes with a sort of *entropic mechanism* near $\rho = 1/2$, where λ_2 does not saturate due to a critical balance of energies. This shows up as an interesting phenomenon: the ground state at $T = 0$ is characterized by

$$\Delta\rho = \begin{cases} 2\rho & \text{for } 0 \leqslant \rho \leqslant 1/4 \\ 1-2\rho & \text{for } 1/4 \leqslant \rho \leqslant 1/2. \end{cases} \tag{22}$$

More explicitly, one obtains from equation (21) that λ_1 is empty for small enough densities, while a sudden change occurs for $\rho = 1/4$, and λ_2 is half filled and the rest of the particles go to λ_1 for larger densities ($\rho \leqslant 1/2$ in any case). On the other hand, equation (21) implies that the tendency of λ_1 towards saturation at a low enough temperature depends on the difference $J_1 - J_2$ as $\Delta\rho = 2\rho - \varepsilon\exp[-4\beta(J_1 - J_2)]$, $J_1 > J_2$.

One may study any mean-field Hamiltonian also. As an illustration, consider $n = 2$ for $H_i(\sigma^i) = -J_i m_i \sum_x s_x$, $i = 1, 2$; here, $s_x \equiv 2\sigma_x - 1$ and $m_i \equiv 2\rho_i - 1$ correspond to the more familiar Ising formalism. One obtains

$$\beta f_i(\beta, \rho_i) = -\beta J_i(2\rho_i - 1)^2 + \rho_i \ln \rho_i + (1-\rho_i)\ln(1-\rho_i) + \ln 2, \tag{23}$$

and equation (13) transforms into

$$(1-\rho_2)\rho_1/[(1-\rho_1)\rho_2] = \exp\{4\beta[J_1(2\rho_1 - 1) - J_2(2\rho_2 - 1)]\}.$$

The total density is $\rho = u\rho_1 + (1-u)\rho_2$, i.e., $p_1 = u$ and $p_2 = 1-u$, in general. Then, $\rho_1 = \rho_2 = \rho$ holds for any ρ as long as $J_1 = J_2$, or $\beta \to 0$ if $J_1 \neq J_2$; moreover, one has $\rho_1 = \rho_2 = 1/2$ for $J_1 \neq J_2$ if $\rho = 1/2$. Of course, the system may exhibit also solutions $\rho_1 \neq \rho_2$. If $J_1 = J_2$, local stability of $\rho_1 = \rho_2 = 1/2$ breaks down at a temperature $T_C = 8\rho(1-\rho)$ for any u. As expected, one obtains classical critical behaviour $\rho_i - \rho \approx B_i(T - T_C)^{1/2}$, $i = 1, 2$, if either $\rho = 1/2$ or else $u = 1/2$.

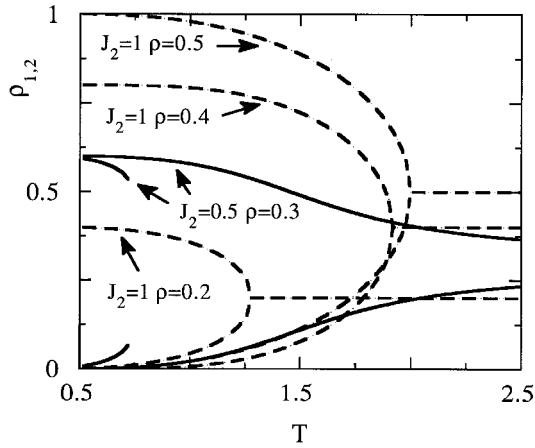

Figure 8. The variation with temperature of the densities of particles ρ_1 (upper line of each $\supset$-shaped curve) and ρ_2 (lower line), within the two lattices of the mean-field system $\Lambda_{d,d}$ in section 4, for $J_1 = 1$, and $p_1 = p_2 = u = 1/2$. Different values for J_2 and ρ are as indicated.

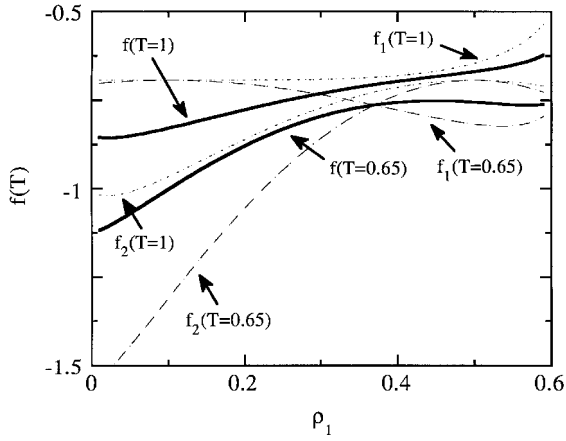

Figure 9. The free energy functions for the system in figure 8, and for each of the boxes (section 5) for $J_2 = 1/2$ and $\rho = 0{\cdot}3$, for several values of the temperature.

Figure 8 depicts the behaviour of $\rho_1(T)$ and $\rho_2(T)$ for $J_1 = 1$, $u = 1/2$, and some representative values of J_2 and ρ. In as long as $J_1 = J_2$, the high temperature phase corresponds to an even distribution of particles between the two boxes, as expected. At $T = T_C = 8\rho(1-\rho)$, the system exhibits a second-order phase transition. As $T \to 0$, the minority species segregates within one of the boxes, and the species of greater density fills up the rest, i.e., $\rho_1 \to 2\rho$ and $\rho_2 \to 0$ for $\rho \leqslant 1/2$. For $J_1 \neq J_2$, no phase transition occurs at any fine temperature but ρ_1 and ρ_2 tend to each other as $T \to \infty$. Analysis of equation (23) indicates that one of the boxes tends to attract particles more than the other but no symmetry to be broken exists, as in the Ising model under non-zero field. As depicted by figure 9, metastable solutions occur for $J_1 \neq J_2$ at low enough T; they disappear discontinuously at $T = 0{\cdot}73$, where $\rho_1 \approx 0{\cdot}52$ and $\rho_2 \approx 0{\cdot}08$, for $\rho = 0{\cdot}3$ and $J_1 = 2J_2 = 1$. This is similar to the metastable-like behaviour reported above for MC experiments (where $J_1 = J_2$, however).

The case $J_1 = J_2 = 1$ with $u \neq 1/2$ is remarkable also. For $\rho = 1/2$, one has $f(\rho_1) = uf_1(\rho_1) + (1-u)f_1(1-\rho_1)$, which implies that $1-\rho_1$ is a solution together with any ρ_1. (Symmetry occurs also if $u = 1/2$ for any ρ, i.e., ρ_1 and $2\rho - \rho_1$ are twin solutions.) Such symmetry no longer holds for $\rho \neq 1/2$; one of the local minima of the free energy then becomes metastable. Consequently, a phase transition occurs from a homogeneous state to an inhomogeneous one which is unique, non-degenerate, acting as a sort of absorbing state. Three regions of the phase diagram may be defined (figure 9). (i) For $T < T_C = 8\rho(1-\rho)$, the stable solution ρ_1 coexists with a metastable solution, say ρ_1'. As $T \to 0$ one has $\rho_1 \to 1$, and $\rho_1' \to 0$. (ii) The metastable solution has a continuous transition at T_C, and the new metastable solution is $\rho_1' = \rho$. The stable value ρ_1 decreases with increasing T within the range $T_C \leqslant T \leqslant T^*$, and a discontinuity occurs at T^*; one obtains the critical values, e.g., $\rho_1^c(u = 0{\cdot}4) \approx 0{\cdot}47$ and $\rho_1^c(u = 0{\cdot}2) \approx 0{\cdot}54$. (iii) The system has a unique stable, *homogeneous* solution, i.e., $\rho_1 = \rho$, for $T > T^*$. One obtains, for instance, $T^* \approx 1{\cdot}93$ for $u = \rho = 0{\cdot}4$, and $T^* \approx 1{\cdot}54$ for $u = \rho = 0{\cdot}2$.

5. Conclusion

We have studied some simple cases of $\Lambda \equiv \bigcup_i \lambda_i$ which is not always simply related to the ordinary lattice gas λ. This is a consequence of the balance between the free energies of the boxes λ that are coupled non-trivially in Λ by chemical potentials. It is remarkable that varied and interesting behaviour may be expected for lattices of different volume, $|\lambda_1| \neq |\lambda_2| \ldots$, and interaction strength, $J_1 \neq J_2 \ldots$. The simplest case, $\Lambda_{1,1,\ldots}$, which consists of n equal lines, may be solved exactly (section 4). In particular, equation (21) describes a transition at zero temperature as a function of ρ for $n = 2$ in which one of the lines is empty for $\rho \leqslant 1/4$, and changes over to density $2\rho - 1/2$ for $1/2 \leqslant \rho \leqslant 1/4$. A phenomenon which is similar in a sense occurs at finite temperatures in $\Lambda_{2,2}$. There is phase segregation in only one of the planes below $T_C(\rho)$ which satisfies equations (1)–(3). It has some interesting consequences which have been discussed in sections 2 and 3. One may devise simple variations of Λ for which we did not find any relation with λ; it suggests that studying further variations of Λ is interesting by itself.

Although we have not investigated such a possibility here, it is clear that some variations of Λ may be of practical interest. In particular, $\Lambda_{2,2}$ may model quasi two-dimensional ionic conduction which occurs in certain solid electrolytes if provided with an external dissipative electric field driving the particles [10]. Another remarkable feature of Λ that endows it with practical interest is that density fluctuations do not need to decay necessarily via diffusion (in the same lattice) due to the existence of further (uncoupled) lattices (figures 4 and 6). It has been shown to help the study of coexistence of phases, and it may be interesting for computer simulations of nucleation and spinodal decomposition, for instance. In particular, some of the advantages of the Gibbs ensemble for the study of, e.g., phase equilibrium of mixtures, etc., may also hold for Λ, which seems computationally preferable.

We acknowledge very useful comments by Giovanni Gallavoti and Joel L. Lebowitz, and partial financial support from the Dirección General de Investigación Científica y Técnica, Project PB91-0709, and Plan Andaluz de Investigación, Junta de Andalucía, of Spain.

References

[1] YANG, C. N., and LEE, T. D., 1952, *Phys. Rev.*, **87**, 404, 410.
[2] See, e.g. BINDER, K., 1984, *Applications of the Monte Carlo Method in Statistical Physics* (Berlin: Springer-Verlag), and references therein.
[3] PANAGIOTOPOULOS, A. Z., 1987. *Molec. Phys.*, **61**, 812.
[4] AMAR, J. G., 1989, *Molec. Phys.*, **67**, 739.
[5] SMIT, B., SMEDT, P., and FRENKEL, D., 1989, *Molec. Phys.*, **68**, 931.
[6] PANAGIOTOPOULOS, A. Z., 1992, *Molec. Simulation*, **9**, 1.
[7] MON, K. K., 1993, *Phys. Rev.* B, **47**, 5497, and references therein.
[8] ROVERE, M., NIELABA, P., and BINDER, K., 1993, *Z. Phys.* B, **90**, 215.
[9] HANSEN, P. L., LEMMICH, J., IPSEN, J. H., and MOURITSEN, O. G., 1993, *J. statist. Phys.*, **73**, 723.
[10] ACHAHBAR, A., and MARRO, J., 1995, *J. statist. Phys.*, **78**, 1493.
[11] ONSAGER, L., 1944, *Phys. Rev.*, **65**, 117.
[12] MIRACLE SOLÉ, S., 1976, *Critical Phenomena*, edited by J. Brey and R. B. Jones. (Heidelberg: Springer-Verlag), p. 197.
[13] WANG, J. S., BINDER, K., and LEBOWITZ, J. L., 1989, *J. statist. Phys.*, **56**, 783.